KaVA Status Report for 2019B

KaVA User Support Team, NAOJ and KASI

April 15, 2019

Major revision since 2019B

- New mode for KaVA K-band astrometry (see Appendixes C and D)
- Contact e-mail addresses are changed (see Table 11)

Contents

1	Intr	roduction	4
2	Sys	tem	5
	2.1	Array	5
	2.2	Antennas	6
		2.2.1 Brief Summary of VERA Antennas	6
		2.2.2 Brief Summary of KVN Antennas	6
		2.2.3 Aperture Efficiency	7
		2.2.4 Beam Pattern and Size	8
	2.3	Receivers	9
		2.3.1 Brief Summary of VERA Receiving System	9
		2.3.2 Brief Summary of KVN Receiving System	10
	2.4	Digital Signal Process	15
	2.5	Recorders	15
	2.6	Correlators	15
	2.7	Calibration	16
		2.7.1 Delay and Bandpass Calibration	16
		2.7.2 Gain Calibration	16
	2.8	Geodetic Measurement	17
		2.8.1 Brief Summary of VERA Geodetic Measurement	17
		2.8.2 Brief Summary of KVN Geodetic Measurement	18
3	Obs	serving Proposal	19
	3.1	Call for Proposal (CfP)	19
	3.2	Proposal Submission	19
	3.3	Observation Mode	20
	3.4	Possible Conflict/duplication with KaVA Large Programs	20
	3.5	Target of Opportunity (ToO) Observations	20
	3.6	Angular Resolution and Largest Detectable Angular Scale	20
	3.7	Sensitivity	21
	3.8	Calibrator Information	22
	3.9	Date Archive	23
	3.10	Recovery Observation	23
4	Obs	servation and Data Reduction	24
	4.1	Preparation	24
	4.2	Observation and Correlation	24
	4.3	Data Reduction	24

	4.4	Further Information	25
A	New	observation mode from 2016B	26
	A.1	Fast antenna nodding mode	26
	A.2	1-beam hybrid (K/Q/W) mode	26
В	New	observation mode from 2018A	27
	B.1	C2 mode at Q-band	27
	B.2	Wide-field imaging mode	27
\mathbf{C}	New	observation mode from 2019A	29
	C.1	Phase referencing mode at K-band	29
		C.1.1 VERA dual-beam and KVN single-beam observations	29
		C.1.2 Tropospheric calibration with GPS and JMA data	30
		C.1.3 Delay recalculation table for precise position measurement	31
		C.1.4 Digital filter mode	31
		C.1.5 Data reduction	31
		C.1.6 Note	32
D	New	observation mode from 2019B	33
	D.1	K-band astrometry mode for parallax and proper motion measurements	33
	D.2	C2 mode at K-band	35

1 Introduction

This document summarizes the current observational capabilities of KaVA (KVN and VERA Array), which is a combined VLBI network of KVN (Korean VLBI Network) and VERA (VLBI Exploration of Radio Astrometry) operated by Korea Astronomy and Space Science Institute (KASI) and National Astronomical Observatory of Japan (NAOJ), respectively (see Figure 1).

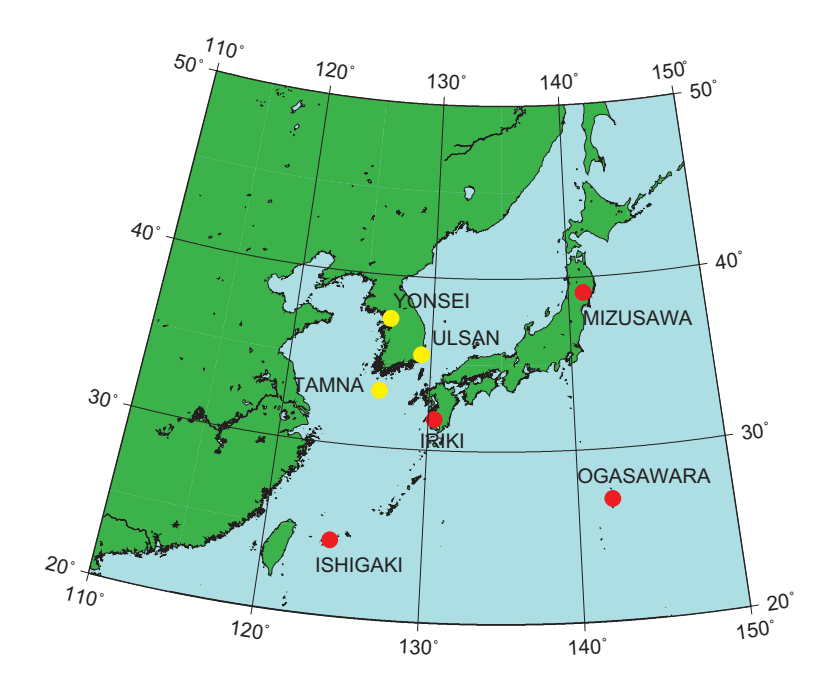


Figure 1: Array configuration of KaVA.

VERA is a Japanese VLBI array to explore the 3-dimensional structure of the Milky Way Galaxy based on high-precision astrometry of Galactic maser sources. VERA array consists of four 20 m radio telescopes located at Mizusawa, Iriki, Ogasawara, and Ishigakijima with baseline ranges from 1000 km to 2300 km. The construction of VERA array was completed in 2002, and it is under regular operation since the fall of 2003. VERA was opened to international users in the K band (22 GHz) and Q band (43 GHz) from 2009. Most unique aspect of VERA is "dual-beam" telescope, which can simultaneously observe nearby two sources. While single-beam VLBI significantly suffers from fluctuation of atmosphere, dual-beam observations with VERA effectively cancel out the atmospheric fluctuations, and then VERA can measure relative positions of target sources to reference sources with higher accuracy based on the 'phase-referencing' technique. For more detail, visit the following web site:

http://veraserver.mtk.nao.ac.jp/index.html.

KVN is the mm-wavelength VLBI facility in Korea. It consists of three 21 m radio telescopes, which are located in Seoul (Yonsei University), Ulsan (University of Ulsan), and Jeju island (ex-Tamna University), and produces an effective spatial resolution equivalent to that of a 500 km radio telescope. KASI has developed innovative multi-frequency band receiver systems, observing four different frequencies at 22, 43, 86, and 129 GHz simultaneously. With this capability, KVN will provide opportunities to study the formation and death processes of stars, the structure and dynamics of our

own Galaxy, the nature of Active Galactic Nuclei and so on at milli-arcsecond (mas) resolutions. For more detail, visit the following web site and paper (Lee et al. 2011):

KaVA was formed in 2010, on the basis of the VLBI collaboration agreement between KASI and NAOJ. KaVA complements baseline length range up to 2270 km, and can achieve a good imaging quality. Currently, KaVA supports observations at K band and Q band in left-hand-circular polarization with a data aggregation rate of 1024 Mega bit per seconds (bps) (=1 Gbps). This document is intended to give astronomers necessary information for proposing observations with KaVA. For more detail, visit the following web site:

http://kava.kasi.re.kr.

In 2014, the first results from KaVA have been published. Matsumoto et al. (2014) report the first VLBI detection of the 44 GHz methanol maser emission associated with a massive star-forming region (SFR). They demonstrate the unique capability of KaVA to image extended maser features. Niinuma et al. (2014) report the detailed analysis of KaVA observations of active galactic nuclei (AGN). The paper discuss about imaging quality and flux calibration accuracy of KaVA. In 2016, the new papers on maser emission around an asymptotic giant branch (AGB) star WX PSc was published (Yun et al. 2016). These three papers are based on the initial results from KaVA large programs started since 2016, demonstrating high capabilities of KaVA for SFR, AGN, and AGB projects.

2 System

2.1 Array

KaVA consists of 7 antenna sites in VERA-Mizusawa, VERA-Iriki, VERA-Ogasawara, VERA-Ishigakijima, KVN-Yonsei, KVN-Ulsan and KVN-Tamna with 21 baselines (see Figure 1). The maximum baseline length is 2270 km between Mizusawa and Ishigakijima, and the minimum baseline length is 305 km between Yonsei and Ulsan. The maximum angular resolution expected from the baseline length is about 1.2 mas for K band and about 0.6 mas for Q band. The geographic locations and coordinate of each KaVA antenna in the coordinate system of epoch 2009.0 are summarized in Table 1. The geographic locations and coordinate of each KaVA antenna are summarized in Table 1. Figure 2 shows examples of uv plane coverage.

The coordinates and averaged velocities of VERA sites in Table 2 are predicted values at the epoch of January 01, 2018. Reference frame of these coordinates is ITRF2014. The rates of the coordinates of Mizusawa, Iriki, Ogasawara and Ishigakijima are the average value of change of the coordinates from April 16, 2016 to May 26, 2018, after the 2016 Kumamoto Earthquake (Mj 7.3). The 2011 off the Pacific coast of Tohoku Earthquake (Mj=9.0) brought the co-seismic large step and non-linear post-seismic movement to the coordinates of Mizusawa. Co-seismic steps of the coordinates of Mizusawa are dX=-2.0297m, dY=-1.4111m and dZ=-1.0758m. The creeping continues still now, though decreased. The changes of coordinates by the post-seismic creeping are dX=-0.8574m, dY=-0.5387m and dZ=-0.2398m in total from March, 12, 2011 to Jan, 01, 2015.

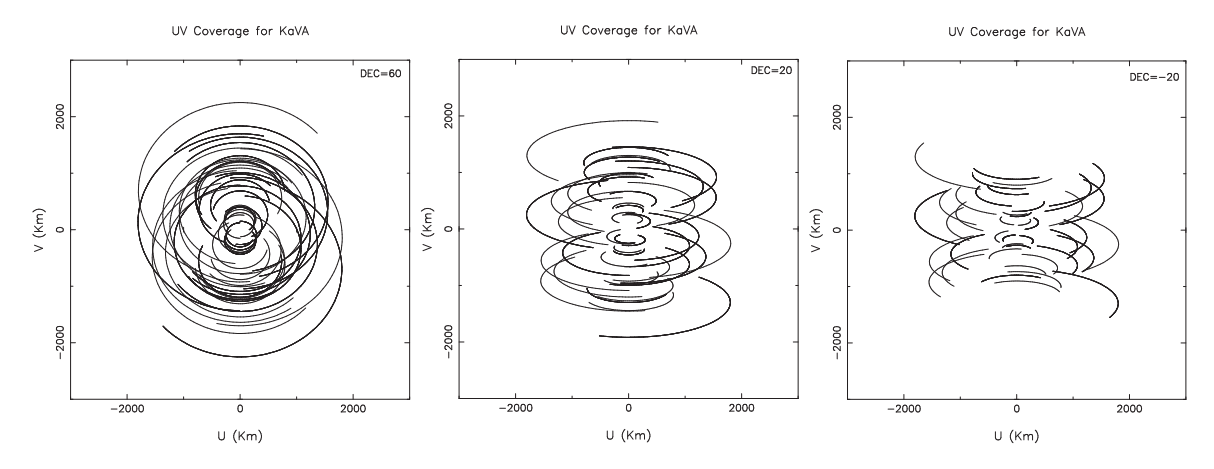


Figure 2: The uv plane coverage (± 3000 km) expected with KaVA antennas from an observation over elevation of 20°. Each panel shows the uv coverage for the declination of 60° (left), 20° (center), and -20° (right).

In the case of KVN, all antenna locations are measured with GPS system. The antenna positions of KVN are regularly monitored both with GPS system and geodetic VLBI observations in collaboration with VERA. No velocity information is available for KVN stations.

2.2 Antennas

2.2.1 Brief Summary of VERA Antennas

All the telescopes of VERA have the same design, being a Cassegrain-type antenna on AZ-EL mount. Each telescope has a 20 m diameter dish with a focal length of 6 m, with a sub-reflector of 2.6 m diameter. The dual-beam receiver systems are installed at the Cassegrain focus. Two receivers are set up on the Stewart-mount platforms, which are sustained by steerable six arms, and with such systems one can simultaneously observe two adjacent objects with a separation angle between 0.32 and 2.2 deg. The whole receiver systems are set up on the field rotator (FR), and the FR rotate to track the apparent motion of objects due to the earth rotation. Table 3 summarizes the ranges of elevation (EL), azimuth (AZ) and field rotator angle (FR) with their driving speeds and accelerations. In the case of single beam observing mode, one of two beams is placed at the antenna vertex (separation offset of 0 deg).

2.2.2 Brief Summary of KVN Antennas

The KVN antennas are also designed to be a shaped-Cassegrain-type antenna with an AZ-EL mount. The telescope has a 21 m diameter main reflector with a focal length of 6.78 m. The main reflector consists of 200 aluminum panels with a manufacturing surface accuracy of about 65 μ m. The slewing speed of the main reflector is 3 °/sec, which enables fast position-switching observations (Table 3). The sub-reflector position, tilt, and tip are remotely controlled and modeled to compensate for the gravitational deformation of the main reflector and for the sagging-down of the sub-reflector itself.

Table 1: Geographic locations and motions of each KaVA antenna.

	East	North	Ellipsoidal			
	Longitude	Latitude	Height	X^a	Y^a	Z^a
Site	[°′″]	[° ′ ′′]	[m]	[m]	[m]	[m]
Mizusawa	141 07 57.34	$39\ 08\ 00.67$	116.6	-3857244.9089	3108782.9415	4003899.1770
Iriki	$130\ 26\ 23.60$	$31\ 44\ 52.43$	573.6	-3521719.8633	4132174.6847	3336994.1305
Ogasawara	$142\ 12\ 59.79$	$27\ 05\ 30.49$	273.1	-4491068.4253	3481545.2331	2887399.7871
Ishigaki	$124\ 10\ 15.59$	$24\ 24\ 43.81$	65.1	-3263995.2318	4808056.3788	2619948.6690
$Yonsei^b$	$126\ 56\ 27.4$	$37\ 33\ 54.9$	139	-3042280.9137	4045902.7164	3867374.3544
$Ulsan^b$	$129\ 14\ 59.3$	$35\ 32\ 44.2$	170	-3287268.7200	4023450.0790	3687379.9390
Tamna^b	$126\ 27\ 34.4$	$33\ 17\ 20.9$	452	-3171731.7246	4292678.4575	3481038.7330

^aThe epoch of the coordinates of VERA is January, 01, 2015.

Table 2: Station code and average velocity of each VERA antenna.

Site	$IVS2^a$	$IVS8^b$	CDP^c	$\Delta X [m/yr]^d$	$\Delta Y [m/yr]^d$	$\Delta Z [m/yr]^d$		
Mizusawa	Vm	VERAMZSW	7362	-0.0123	0.0359	-0.0166		
Iriki	Vr	VERAIRIK	7364	-0.0151	0.0038	-0.0105		
Ogasawara	Vo	VERAOGSW	7363	0.0378	0.0298	0.0183		
Ishigakijima	Vs	VERAISGK	7365	-0.0332	-0.0074	-0.0471		

^aIVS 2-characters code

2.2.3 Aperture Efficiency

The aperture efficiency of each VERA antenna is about 40–50% in both K band and Q band (see Table 4 for the 2019 and 2012 data for VERA and KVN, respectively). The latest values for VERA were measured from 2018 December to 2019 March. These measurements were based on the observations of Jupiter assuming that the brightness temperature of Jupiter is 160 K in both the K band and the Q band. Due to the bad weather condition in some of the sessions, the measured efficiencies show large scatter. However, we conclude that the aperture efficiencies are not significantly changed compared with previous measurements. The elevation dependence of aperture efficiency for VERA antenna was also measured from the observation toward maser sources. Fig-

Table 3: Driving performance of KaVA antennas.

<u> </u>								
Driving axis	Driving range Max. driving spee		Max. driving acceleration					
		VERA						
$\overline{\mathrm{AZ}^a}$	$-90^{\circ} \sim 450^{\circ}$	$2.1^{\circ}/\text{sec}$	$2.1^{\circ}/\mathrm{sec}^2$					
EL	$5^{\circ} \sim 85^{\circ}$	$2.1^{\circ}/\mathrm{sec}$	$2.1^{\circ}/\mathrm{sec}^2$					
FR^b	$-270^{\circ} \sim 270^{\circ}$	$3.1^{\circ}/\mathrm{sec}$	$3.1^{\circ}/\mathrm{sec^2}$					
		KVN						
AZ^a	$-90^{\circ} \sim 450^{\circ}$	3°/sec	$3^{\circ}/\mathrm{sec}^2$					
EL	$5^{\circ} \sim 85^{\circ}$	$3^{\circ}/\mathrm{sec}$	$3^{\circ}/\mathrm{sec}^2$					

^aThe north is 0° and the east is 90° .

^bThe KVN antenna positions are obtained by the KaVA K-band geodesy program on January 24, 2014.

 $[^]b {
m IVS}$ 8-characters code

^cCDP (NASA Crustal Dynamics Project) code

^dThe epoch of the coordinates is January 01, 2015. Average speed was obtained from the VLBI data from January 01, 2014 to June 10, 2016.

 $[^]b\mathrm{FR}$ is 0° when Beam-1 is at the sky side and Beam-2 is at the ground side, and CW is positive when an antenna is seen from a target source.

Table 4: Apertu	re efficiency	and beam	size of	KaVA	antennas.

		<i>J</i>		
	K band (22 GHz)		Q ban	d (43 GHz)
	$\eta_{ m A}$	$\eta_{\rm A}$ HPBW		HPBW
Antenna Name	(%)	(arcsec)	(%)	(arcsec)
Mizusawa	48	139	50	68
Iriki	45	136	41	72
Ogasawara	41	134	43	72
Ishigakijima	47	141	47	73
Yonsei	55	127	63	63
Ulsan	63	124	61	63
Tamna	60	126	63	63

ures 3 shows the relations between the elevation and the aperture efficiency measured for VERA Iriki station. The gain curves are measured by observing the total power spectra of intense maser sources. The aperture efficiency in low elevation of ≤ 20 deg decreases slightly, but this decrease is less than about 10%. Concerning this elevation dependence, the observing data FITS file include a gain curve table (GC table), which is AIPS readable, in order to calibrate the dependence when the data reduction.

The aperture efficiency and beam size for each KVN antenna are also listed in Table 4. Aperture efficiency of KVN varies with elevation as shown in Figure 3. The main reflector panels of KVN antennas were installed to give the maximum gain at the elevation angle of 48°. The sagging of sub-reflector and the deformation of main reflector by gravity with elevation results in degradation of antenna aperture efficiency with elevation. In order to compensate this effect, KVN antennas use a hexapod to adjust sub-reflector position. Figure 3 shows the elevation dependence of antenna aperture efficiency of the KVN 21 m radio telescopes measured by observing Venus or Jupiter. By fitting a second order polynomial to the data and normalizing the fitted function with its maximum, we derived a normalized gain curve which has the following form:

$$G_{\text{norm}} = A_0 E L^2 + A_1 E L + A_2,$$
 (1)

where EL is the elevation in degree.

2.2.4 Beam Pattern and Size

Figure 4 shows the beam patterns in the K band. The side-lobe level is less than about -15 dB, except for the relatively high side-lobe level of about -10 dB for the separation angle of 2.0 deg at Ogasawara station. The side-lobe of the beam patterns has an asymmetric shape, but the main beam has a symmetric Gaussian shape without dependence on separation angle. The measured beam sizes (HPBW) in the K band and the Q band based on the data of the pointing calibration are also summarized in Table 4. The main beam sizes show no dependence on the dual-beam separation angle.

The optics of KVN antenna is a shaped Cassegrain type of which the main reflector and subreflector are shaped to have a uniform illumination pattern on an aperture plane. Because of the uniform illumination, KVN antennas can get higher aperture efficiency than value of typical Cassegrain type antenna. However, higher side-lobe level is inevitable. OTF images of Jupiter at K and Q bands are shown in Figure 4. The map size is 12'×10' and the first side-lobe pattern is clearly visible. Typical side-lobe levels of KVN antennas are 13-14dB.

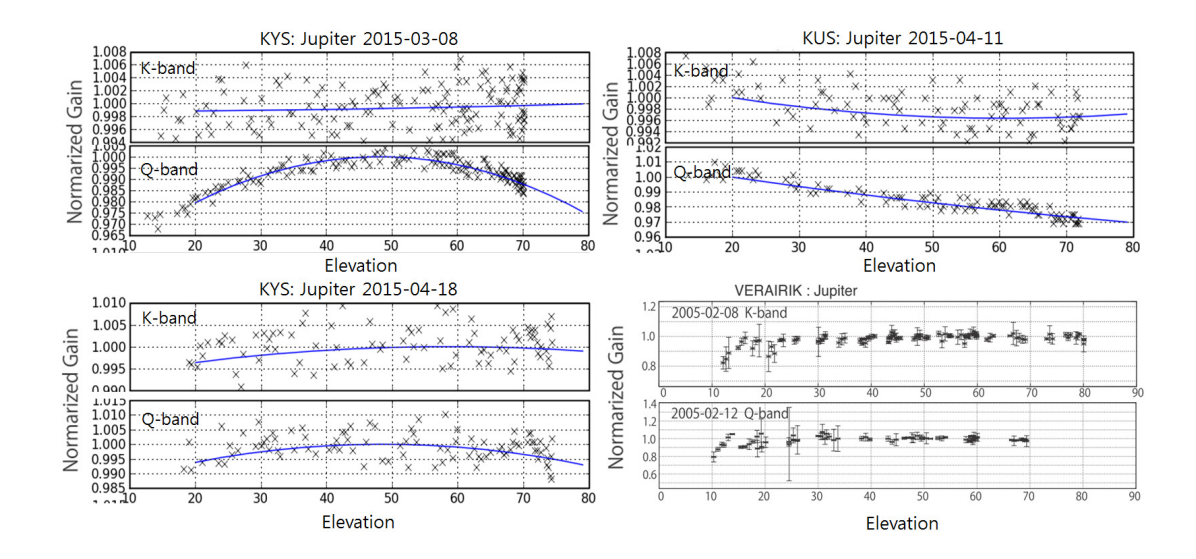


Figure 3: The elevation dependence of the aperture efficiency for KVN three antennas and VERA Iriki antenna. For KVN antennas, the maximum gain is given at the elevation angle of 48°. The efficiency in K-band (on Feb 8, 2005) and the Q-band (on Feb 12, 2005) for VERA Iriki antenna is shown in *bottom right*. The efficiency is relative value to the measurement at $EL = 50^{\circ}$.

2.3 Receivers

2.3.1 Brief Summary of VERA Receiving System

Each VERA antenna has the receivers for 4 bands, which are S (2 GHz), C (6.7 GHz), X (8 GHz), K (22 GHz), and Q (43 GHz) bands. For the open use, the K band and the Q band are open for observing. The low-noise HEMT amplifiers in the K and Q bands are enclosed in the cryogenic dewar, which is cooled down to 20 K, to reduce the thermal noise. The range of observable frequency and the typical receiver noise temperature $(T_{\rm RX})$ at each band are summarized in the Table 5 and Figure 5.

Table 5: Frequency range and T_{RX} of <u>VERA and KVN receivers</u>.

	Frequency Range	$T_{\rm RX}{}^a$					
Band	[GHz]	[K]	Polarization				
	VERA						
K	21.5-23.8	30-50	LCP				
Q	42.5 - 44.5	70-90	LCP				
		KVN					
K	18-26	20-40	LCP/RCP				
Q	42.11 - 44.11	70-80	LCP/RCP				
		(40-50 for Ulsan)					

^aReceiver noise temperature

After the radio frequency (RF) signals from astronomical objects are amplified by the receivers, the RF signals are mixed with standard frequency signal generated in the first local oscillator to down-convert the RF to an intermediate frequency (IF) of 4.7 GHz–7 GHz. The first local frequencies are fixed at 16.8 GHz in the K band and at 37.5 GHz in the Q band. The IF signals are then mixed down again to the base band frequency of 0–512 MHz. The frequency of second local oscillator is tunable

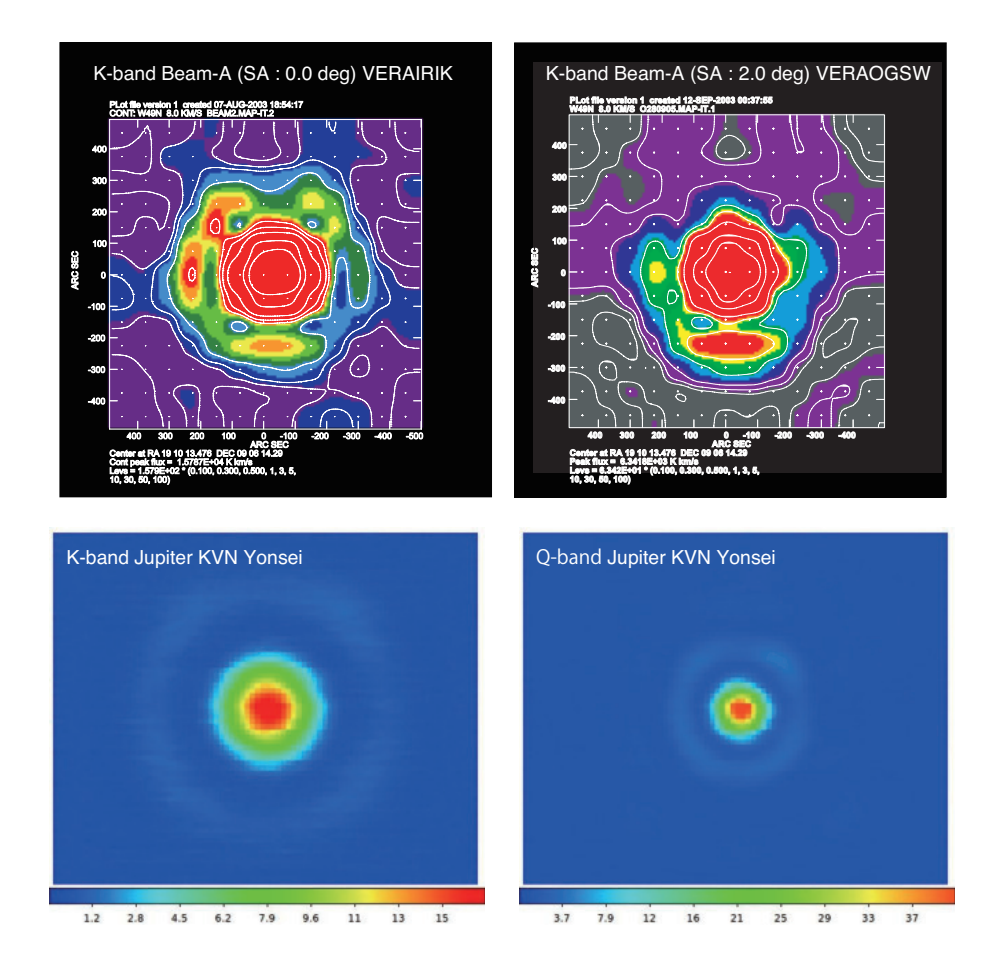


Figure 4: The beam patterns in the K-band for VERA (A-beam) Iriki with the separation angle of 0° (*Upper left*) and Ogasawara with the separation angle of 2.0° (*Upper right*), and in K/Q-band for KVN Yonsei. The patterns of VERA antennas were derived from the mapping observation of strong H₂O maser toward W49N, which can be assumed as a point source, with grid spacing of 75". In the case of KVN antennas, the patterns were derived from the OTF images of Venus at K/Q-band.

with a possible frequency range between 4 GHz and 7 GHz. The correction of the Doppler effect due to the earth rotation is carried out in the correlation process after the observation. Therefore, basically the second local oscillator frequency is kept to be constant during the observation. Figure 6 shows a flow diagram of these signals for VERA.

2.3.2 Brief Summary of KVN Receiving System

The KVN quasi-optics are uniquely designed to observe 22, 43, 86 and 129 GHz band simultaneously (Han et al. 2008, 2013). Figure 7 shows the layout of quasi-optics and receivers viewing from sub-reflector side. The quasi-optics system splits one signal from sub-reflector into four using three dichroic low-pass filters marked as LPF1, LPF2 and LPF3 in the Figure 7. The split signals into four different frequency bands are guided to corresponding receivers.

Figures 8 shows a signal flows in KVN system. The 22, 43 and 86 GHz band receivers are cooled HEMT receivers and the 129 GHz band receiver is a SIS mixer receiver. All

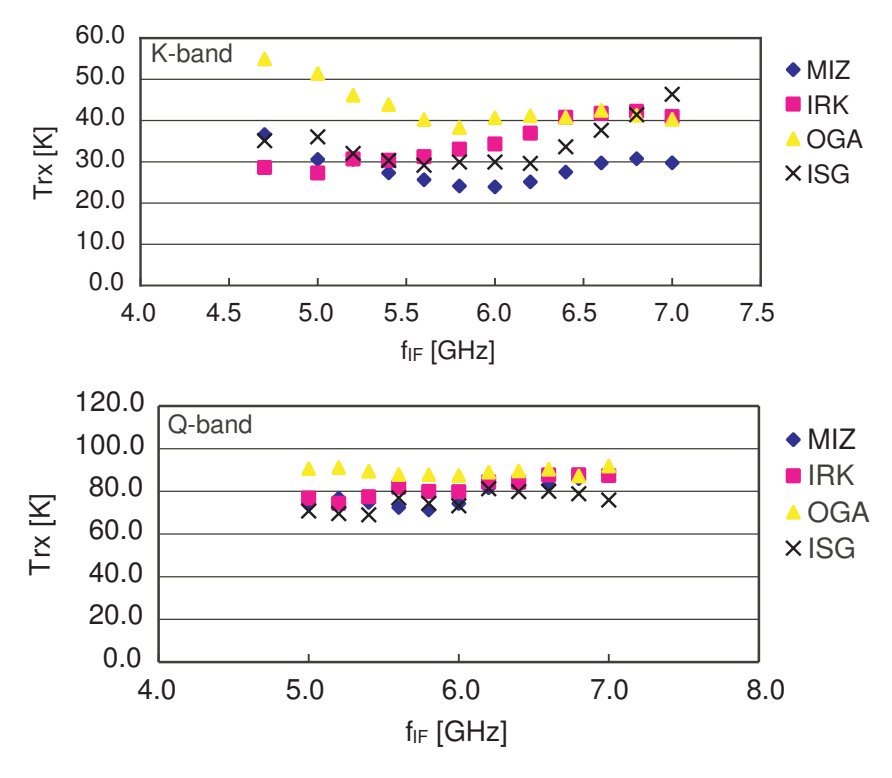


Figure 5: Receiver noise temperature for each VERA antenna. Top and bottom panels show measurements in the K and Q bands, respectively. Horizontal axis indicate an IF (intermediate frequency) at which $T_{\rm RX}$ is measured. To convert it to RF (radio frequency), add 16.8 GHz in the K band and 37.5 GHz in the Q band to the IF frequency.

receivers receive dual-circular-polarization signals. Among eight signals (four dual-polarization signals), four signals selected by the IF selector are down-converted to the input frequency band of the sampler. The instantaneous bandwidth of the 1st IF of each receiver is limited to 2 GHz by the band-pass filter. The 1st IF signal is down-converted by BBCs to the sampler input frequency (512-1024 MHz) band.

Typical noise temperatures of K and Q bands are presented in Table 5. Since the calibration chopper is located before the quasi-optics as shown in Figure 7, the loss of quasi-optics contributes to receiver noise temperature instead of degrading antenna aperture efficiency. Therefore, the noise temperature in the table includes the contribution due to the quasi-optics losses.

The receiver noise temperatures of three stations are similar to each other except that the noise temperature of the Ulsan 43 GHz because of the different type of thermal isolator, which is used to reduce heat flow from the feed horn in room temperature stage to cryogenic cooled stage more effectively.

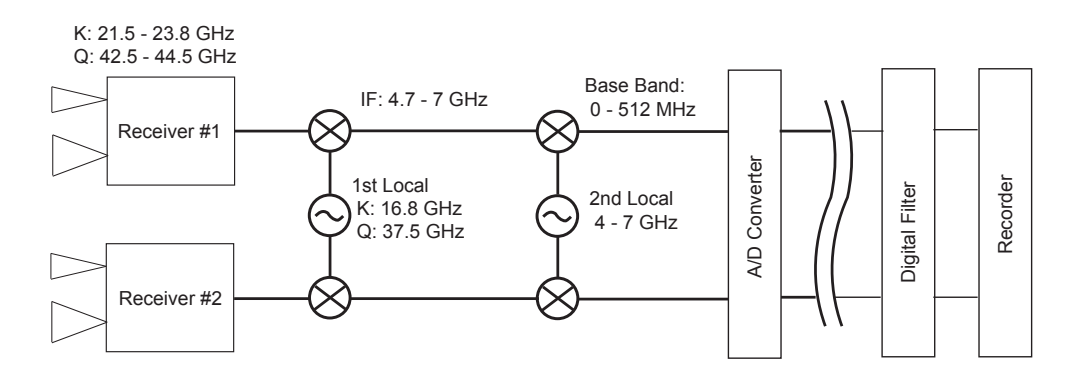


Figure 6: Flow diagram of signals from receiver to recorder for VERA.

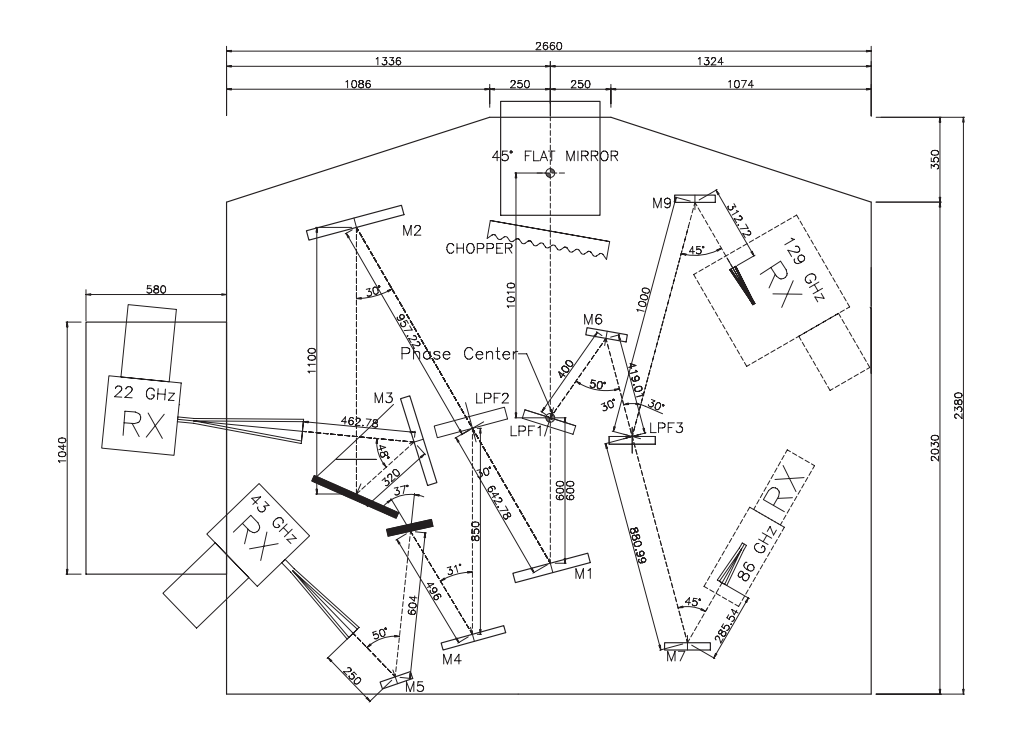


Figure 7: KVN multi-frequency receiving system (Han et al. 2008, 2013).

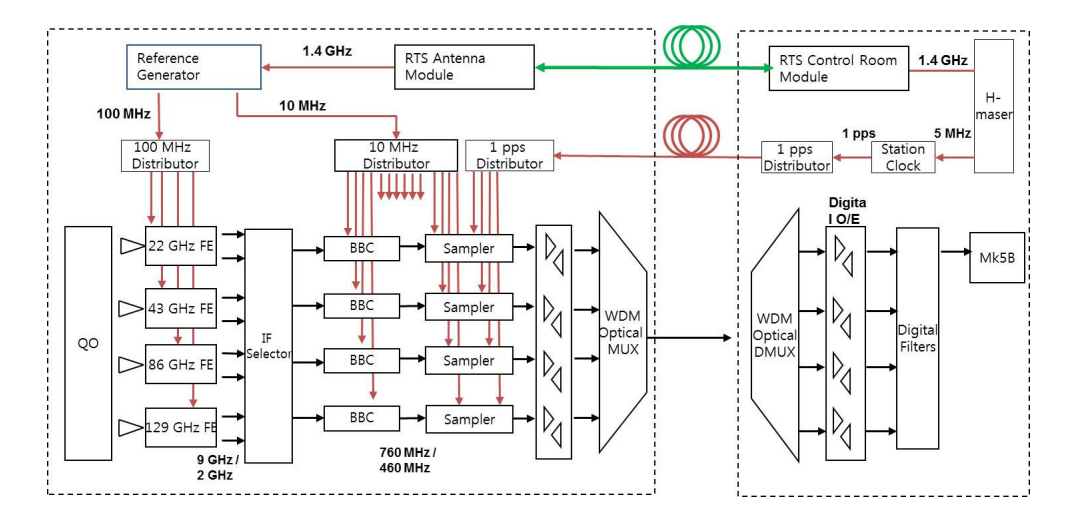


Figure 8: Flow diagram of signals from receiver to recorder for KVN (Oh et al. 2011).

Table 6: Digital filter mode for KaVA.

Name (Mb) GEO1K* 102 GEO1S* 102	24	16 CH ^a	(MHz) 16	CH ^c 1 2 3 4 5 6 7 8 9 10 11 12 13 14 15	(MHz) 0 - 16 32 - 48 64 - 80 96 - 112 128 - 144 160 - 176 192 - 208 224 - 240 256 - 272 288 - 304 320 - 336 352 - 368 384 - 400 416 - 432 448 - 464	Band ^e U U U U U U U U U U U U U U U U U U U	Note ^f Target line (e.g. H ₂ O)
			16	2 3 4 5 6 7 8 9 10 11 12 13 14 15	32 - 48 64 - 80 96 - 112 128 - 144 160 - 176 192 - 208 224 - 240 256 - 272 288 - 304 320 - 336 352 - 368 384 - 400 416 - 432	U U U U U U U U U	Target line (e.g. H_2O)
GEO1S* 102	24	16		3 4 5 6 7 8 9 10 11 12 13 14 15	64 - 80 96 - 112 128 - 144 160 - 176 192 - 208 224 - 240 256 - 272 288 - 304 320 - 336 352 - 368 384 - 400 416 - 432	U U U U U U U U U	Target line (e.g. H_2O)
GEO1S* 102	24	16		4 5 6 7 8 9 10 11 12 13 14 15	96 - 112 128 - 144 160 - 176 192 - 208 224 - 240 256 - 272 288 - 304 320 - 336 352 - 368 384 - 400 416 - 432	U U U U U U U U U	Target line (e.g. H_2O)
GEO1S* 102	24	16		5 6 7 8 9 10 11 12 13 14 15	128 - 144 160 - 176 192 - 208 224 - 240 256 - 272 288 - 304 320 - 336 352 - 368 384 - 400 416 - 432	U U U U U U U U	Target line (e.g. H_2O)
GEO1S* 102	24	16		6 7 8 9 10 11 12 13 14 15	160 - 176 192 - 208 224 - 240 256 - 272 288 - 304 320 - 336 352 - 368 384 - 400 416 - 432	U U U U U U U U	Target line (e.g. H_2O)
GEO1S* 102	24	16		7 8 9 10 11 12 13 14 15	192 - 208 224 - 240 256 - 272 288 - 304 320 - 336 352 - 368 384 - 400 416 - 432	U U U U U U U	Target line (e.g. H_2O)
GEO1S* 102	24	16		8 9 10 11 12 13 14 15	224 - 240 256 - 272 288 - 304 320 - 336 352 - 368 384 - 400 416 - 432	U U U U U U	Target line (e.g. H_2O)
GEO1S* 102	24	16		9 10 11 12 13 14 15	256 - 272 288 - 304 320 - 336 352 - 368 384 - 400 416 - 432	U U U U U	Target line (e.g. H_2O)
GEO1S* 102	24	16		10 11 12 13 14 15	288 - 304 320 - 336 352 - 368 384 - 400 416 - 432	U U U U U	Target line (e.g. H_2O)
GEO1S* 105	24	16		11 12 13 14 15	320 - 336 352 - 368 384 - 400 416 - 432	U U U U	
GEO1S* 10:	24	16		12 13 14 15	352 - 368 384 - 400 416 - 432	U U U	
GEO1S* 102	24	16		13 14 15	384 - 400 416 - 432	U U	
GEO1S* 102	24	16		14 15	416 - 432	U	
GEO1S* 109	24	16		15			
GEO1S* 105	24	16			118 161	T T	
GEO1S* 10:	24	16					
GEO1S* 10:	24	16		16	480 - 496	U	
		10	16	1	112 - 128	L	
				2	128 - 144	U	
				3	144 - 160	L	
				4	160 - 176	U	
				5	176 - 192	L	
				6	192 - 208	U	
				7	208 - 224	L	
				8	224 - 240	U	
				9	240 - 256	L	
				10	256 - 272	U	Target line (e.g. H_2O)
				11	272 - 288	L	
				12	288 - 304	U	
				13	304 - 320	L	
				14	320 - 336	U	
				15	336 - 352	L	
				16	352 - 368	U	
VERA7SIOS* 102	24	16	16	1	32 - 48	U	
				2	64 - 80	U	
				3	80 - 96	L	SiO $(J=1-0, v=2)$
				4	96 - 112	U	
				5	128 - 144	U	
				6	160 - 176	U	
				7	192 - 208	U	
				8	224 - 240	U	
				9	256 - 272	U	
				10	288 - 304	U	
				11	384 - 400	U	SiO $(J=1-0, v=1)$
				12	320 - 336	U	, , , ,
				13	352 - 368	U	
				14	416 - 432	U	
				15	448 - 464	U	
				16	480 - 496	Ü	

^{*}All channels are for A-Beam (VERA) and LCP (VERA/KVN). Mode names are tentative. $^a\mathrm{Total}$ number of channels

 $[^]b\mathrm{Bandwidth}$ per channel in MHz

^cChannel number

 $[^]d\mathrm{Filtered}$ frequency range in the base band (MHz) $^e\mathrm{Side}$ Band (LSB/USB)

fExample of spectral line setting

Table 7: Digital filter mode for KaVA — continued.

Mode	Rate	Num.	$\overline{\mathrm{BW/CH}^b}$		$\frac{\text{KaVA} - \text{col}}{\text{Freq. range}^d}$	Side	
Name	(Mbps)	CH^a	(MHz)	CH^c	(MHz)	Band^e	Note^f
VERA4S*	1024	8	32	1	128 - 160	U	
				2	160 - 192	Ĺ	
				3	192 - 224	U	
				4	224 - 256	L	
				5	256 - 288	U	
				6	288 - 320	${ m L}$	
				7	320 - 352	U	
				8	352 - 384	L	
VERA1S*	1024	2	128	1	128 - 256	L	
				2	256 - 384	U	
$\mathbf{VERA1}^{**}$	1024	2	128	1	256 - 384	U	A-Beam
				2	256 - 384	U	B-Beam
$\mathbf{VERA7}^{**}$	1024	16	16	1	256 - 272	U	A-Beam for target line
				2	128 - 144	U	B-Beam (CH 2-16)
				3	144 - 160	L	
				4	160 - 176	U	
				5	176 - 192	L	
				6	192 - 208	U	
				7	208 - 224	L	
				8	224 - 240	U	
				9	240 - 256	L	
				10	256 - 272	U	
				11	272 - 288	L	
				12 13	288 - 304	$_{ m L}^{ m U}$	
				13 14	304 - 320 320 - 336	U	
				15	336 - 352	L	
				16	352 - 368	U	
VERA7MM**	1024	16	16	1	256 - 272	U	A-Beam for target line
V LICITIVIIVI	1024	10	10	2	32 - 48	U	B-Beam (CH 2-16)
				3	64 - 80	Ü	B Beam (CH 2 10)
				4	96 - 112	Ü	
				5	128 - 144	Ŭ	
				6	160 - 176	U	
				7	192 - 208	U	
				8	224 - 240	U	
				9	256 - 272	U	
				10	288 - 304	U	
				11	320 - 336	U	
				12	352 - 368	\mathbf{U}	
				13	384 - 400	U	
				14	416 - 432	U	
				15	448 - 464	U	
			RA) and LCI	16	480 - 496	U	

^{*}All channels are for A-Beam (VERA) and LCP (VERA/KVN).

** New mode for the phase referencing (see Appendixes C and D).

^aTotal number of channels

 $[^]b{\rm Bandwidth}$ per channel in MHz

 $[^]c$ Channel number

 $[^]d\mathrm{Filtered}$ frequency range in the base band (MHz)

^eSide Band (LSB/USB)

2.4 Digital Signal Process

In VERA system, A/D (analog-digital) samplers convert the analog base band outputs of 0–512 MHz $\times 2$ beams to digital form. The A/D converters carry out the digitization of 2-bit sampling with the bandwidth of 512 MHz and the data rate is 2048 Mbps for each beam.

In KVN system, A/D samplers digitize signals into 2-bit data streams with four quantization levels. The base band output is 512–1024 MHz. The sampling rate is 1024 Mega sample per second (Msps) with 2-bit sampling resulting a 2048 Mbps=2 Gbps data rate at 512 MHz frequency bandwidth. Four streams of 512 MHz band width (2 Gbps data rate) can be obtained in the KVN multi-frequency receiving system simultaneously, which means that the total rate is 8 Gbps.

Since the total data recording rate is limited to 1024 Mbps (see the next section), only part of the sampled data can be recorded onto hard disks. The data rate reduction is done by digital filter system, with which one can flexibly choose number and width of recording frequency bands. Observers can select modes of the digital filter listed in the Table 6. New digital filter modes called VERA4S and VERA1S is available from the 2016A and 2018A seasons, respectively (Table 7). In VERA7SIOS mode in the Table 6, two transitions (v=1 & 2) of SiO maser in the Q band can be simultaneously recorded. From the 2019A KaVA observing season, new digital filter modes of VERA1, VERA7, and VERA7MM are available for dual-beam astrometry with VERA (see Appendix C).

2.5 Recorders

The KaVA observations are basically limited to record with 1024 Mbps data rate. To response 1 Gbps recording, VERA and KVN have OCTADISK and Mark5B recording systems, respectively. OCTADISK and Mark5B are hard disk recording systems developed at NAOJ and Haystack observatory, respectively. A high-speed magnetic tape recorder, DIR-2000, is no longer used. Their total bandwidths are 256 MHz because of 2-bit sampling.

2.6 Correlators

The correlation process is carried out by a VLBI correlator located at KJCC (Korea-Japan Correlation Center) at Daejeon, which has been developed as the KJJVC (Korea-Japan Joint VLBI Correlator) located at KJCC (Korea-Japan Correlation Center) project. Hereafter it is tentatively called "Daejeon correlator". The Daejeon correlator can process the data stream of up to 8192 Mbps from maximum 16 antenna stations at once. Currently the raw observed data of KVN stations are recorded and play-backed with Mark5B, and those of VERA stations are recorded and playbacked with OCTADISK at the data rate of 1024 Mbps. Data formats available in the next observing season are 16 IFs×16 MHz ("C5 mode" in The Daejeon correlator terminology), 8 IFs×32 MHz ("C4 mode"), and 2 IFs×128 MHz ("C2 mode"). The C4 and C2 modes are newly available from the 2016A and 2018A seasons, respectively. Minimum integration times (time resolution) are 0.2048, 0.8192, and 1.6384 seconds for C2, C4, and C5 modes, respectively, and the number of frequency channels within each IF is 8192 for both modes (i.e. maximum frequency resolution is about 1.95 kHz). By default,

the number of frequency channels is reduced to 128 (for continuum) or 512 (for line) via channel integration after correlation. One may put a special request of number of frequency channels to take better frequency resolution. The number of frequency channels can be selected among 512, 1024, 2048, 4096 or 8192. Final correlated data is served as FITS-IDI file.

Specification of The Daejeon correlator is summarized in Table 8.

Table 8: Specification of The Daejeon correlator^a.

Table 6. Specification of The Daejeon correlator.					
Max. number of antennas	16				
correlation mode	C2(128 MHz Bandwidth, 2 stream)				
	C4(32 MHz Bandwidth, 8 stream)				
	C5(16 MHz Bandwidth, 16 stream)				
Max. number of corr./input	120 cross + 16 auto				
Sub-array	$2 \operatorname{case}(12+4, 8+8)$				
Bandwidth	$512 \mathrm{\ MHz}$				
Max. data rate/antenna	2048 Mbps VSI-H(32 parallels, 64MHz clock)				
Max. delay compensation	\pm 36,000 km				
Max. fringe tracking	$1.075~\mathrm{kHz}$				
FFT work length	16+16 bits fixed point for real, imaginary				
Integration time	$25.6~\mathrm{msec} \sim 10.24~\mathrm{sec}$				
Data output channels	8192 channels				
Data output rate	Max. 1.4GB/sec at 25.6msec integration time				

^aFor more details, see

http://kvn.kasi.re.kr/status_report/correlator_status.html.

2.7 Calibration

Here we briefly summarize the calibration procedure of the KaVA data. Basically, most of the post-processing calibrations are done by using the AIPS (Astronomical Image Processing System) software package developed by NRAO (National Radio Astronomical Observatory).

2.7.1 Delay and Bandpass Calibration

The time synchronization for each antenna is kept within 0.1 μ sec using GPS and high stability frequency standard provided by the hydrogen maser. To correct for clock parameter offsets with better accuracy, bright continuum sources with accurately-known positions should be observed at usually every 60–80 minutes during observations. A recommended scan length for calibrators is 5–10 minutes. This can be done by the AIPS task FRING. The calibration of frequency characteristic (bandpass calibration) can be also done based on the observation of bright continuum source. This can be done by the AIPS task BPASS.

2.7.2 Gain Calibration

Both VERA and KVN antennas have the chopper wheel of the hot load (black body at the room temperature), and the system noise temperature can be obtained by measuring the ratio of the sky power to the hot load power (so-called R-Sky method). Thus, the measured system noise temperature is a sum of the receiver noise temperature, spillover temperature, and contribution of the atmosphere (i.e. so-called T_{sys}^* corrected for atmospheric opacity). The hot load measurement can be made before/after any scan. Also, the sky power is continuously monitored during scans, so that one can trace the variation of the system noise temperature. The system noise temperature value can be converted to SEFD (System Equivalent Flux Density) by dividing by the antenna gain in K/Jy, which is derived from the aperture efficiency and diameter of each antenna. For the correlated data from KJCC, T_{sys}^* data (TY table) and antenna gain information (GC table) are provided with the ANTAB-readable format. KJCC makes complete version of ANTAB-readable file and provide it to PI. User support team supports PIs as appropriate. The TY and GC tables can be loaded by the AIPS task ANTAB, and these tables are converted to the SN table by the AIPS task APCAL.

Alternatively, one can calibrate the visibility amplitude by the template spectrum method, in which auto-correlation spectra of a maser source is used as the flux calibrator. This calibration procedure is made by the AIPS task ACFIT (see AIPS HELP for ACFIT for more detail).

Further correction is made for VLBI observations taken with 2-bit (4-level) sampling, for the systematic effects of non-optimal setting of the quantizer voltage thresholds. This is done by the AIPS task ACCOR. Another correction should be applied to recover the amplitude loss, which are attributed to the combination of two steps of 2-bit quantization in the digital filtering at the backend system and characteristics of Daejeon correlator. This is done by multiplying the scaling factor of 1.3 (the best current estimation) [8] in the AIPS task APCAL (adverbs aparm(1) = 1.3, opcode = '', and dofit = 1) or SNCOR (adverbs opcode = 'MULA', and sncorprm(1) = 1.3). The amplitude calibrations with KaVA are accurate to 15% or better at K and Q bands.

2.8 Geodetic Measurement

2.8.1 Brief Summary of VERA Geodetic Measurement

Geodetic observations are performed as part of the VERA project observations to derive accurate antenna coordinates. The geodetic VLBI observations for VERA are carried out in the S/X bands and also in the K band. The S/X bands are used in the domestic experiments with the Geographical Survey Institute of Japan and the international experiments called IVS-T2. On the other hand, the K band is used in the VERA internal experiments. We obtain higher accuracy results in the K band compared with the S/X bands. The most up-to-date geodetic parameters are derived through geodetic analyses.

Non-linear post seismic movement of Mizusawa after the 2011 off the Pacific coast of Tohoku Earthquake continues. The position and velocity of Mizusawa is continuously monitored by GPS. The coordinates in the Table 1 are provisional and will be revised with accumulation of geodetic data by GPS and VLBI.

In order to maintain the antenna position accuracy, the VERA project has three kinds of geodetic observations. The first is participation in JADE (JApanese Dynamic Earth observation by VLBI) organized by GSI (Geographical Survey Institute) and IVS-T2 session in order to link the VERA coordinates to the ITRF2008 (International Terrestrial Reference Frame 2008). Basically Mizusawa station participates in JADE

nearly every month. Based on the observations for four years, the 3-dimensional positions and velocities of Mizusawa station till 09/Mar/2011 is determined with accuracies of 7-9 mm and about 1 mm/yr in ITRF2008 coordinate system. But the uncertainty of several centimeters exists in the position on and after March 11, 2011. The second kind of geodetic observations is monitoring of baseline vectors between VERA stations by internal geodetic VLBI observations. Geodetic positions of VERA antennas relative to Mizusawa antenna are measured from geodetic VLBI observations every two weeks. From polygonal fitting of the six-year geodetic results, the relative positions and velocities are obtained at the precisions of 1-2 mm and 0.8-1 mm/yr till 10/Mar/2011. The third kind is continuous GPS observations at the VERA sites for interpolating VLBI geodetic positions. Daily positions can be determined from 24 hour GPS data. The GPS observations are also used to estimate tropospheric zenith delay of each VERA site routinely. The time resolution of delay estimates is 5 minutes.

2.8.2 Brief Summary of KVN Geodetic Measurement

KVN antenna positions are regularly monitored using GPS and geodetic VLBI observations. The K-band geodesy VLBI program between KVN and VERA has been started in 2011. Current KVN antenna positions (see Figures 9)are obtained from the KaVA K-band geodesy on January 24, 2014. The typical 1-sigma errors of geodetic solutions are about 0.4 cm in X, Y, and Z directions. Based on 22 epoch KaVA K-band geodetic observations from Sep. 2012 to Dec. 2016, uncertainty of KVN antenna positions are ~ 2.38 cm at Yonsei, ~ 2.55 cm at Ulsan and ~ 1.58 cm at Tamna.

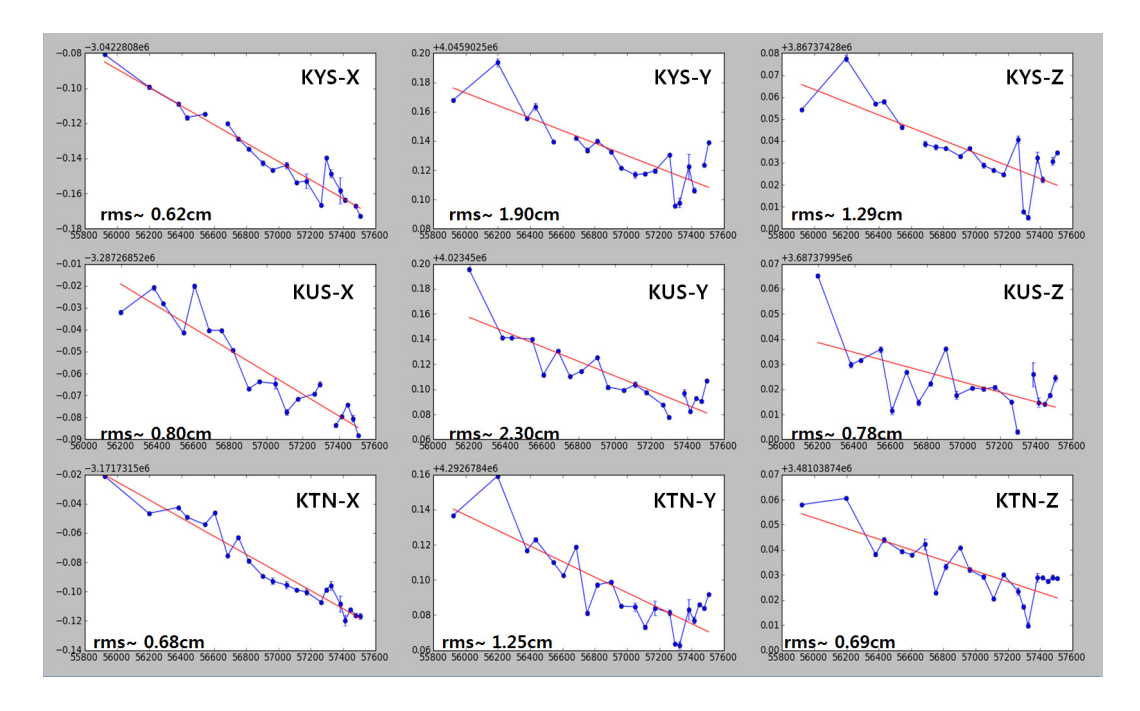


Figure 9: The trend of KVN antenna positions (IVP) in ITRF2014 coordinate system. The x and y axes are MJD and X/Y/Z in meter. The linear fitted is applied to the measurements, shown as red line, and its deviation is also presented in each axis as "rms".

3 Observing Proposal

3.1 Call for Proposal (CfP)

We invite proposals for the open use observations of the KaVA, a joint VLBI array of the KVN (Korean VLBI Network) and the VERA (VLBI exploration of Radio Astrometry). The joint array consists of three 21 m KVN telescopes and four 20 m VERA telescopes, with baseline lengths ranging from 300 km to 2300 km.

This open use call is to provide VLBI observations at 22 GHz and 43 GHz for astronomers around the world. We support astronomers in the preparation of proposals, scheduling, and data analysis. For that reason, proposers who are not familiar with KaVA capability are strongly recommended to consult with KaVA experts prior to submission. If it is difficult to find collaborators from VERA or KVN, please contact us to find one. The contact address for the support is kavaprop (at-mark) kasi.re.kr.

In order to avoid conflicts and/or duplication of the targets between open use proposals and the existing KaVA Large Programs, proposers are highly recommended to visit KaVA Large Program (LP) webpage where KaVA LPs and their source list are presented at

```
http://radio.kasi.re.kr/kava/large_programs.php.
```

Even though the proposed targets are listed in the LPs, they will be accepted as separate open use observations if the scientific goal of the proposals cannot be achieved with the data of the LPs. Otherwise, we encourage the proposers to collaborate with the science teams of the corresponding KaVA LPs.

Observations will be conducted with single polarization (LCP) and 1-Gbps data rate. From this call, KaVA will open phase-referencing observation mode. Please consult the KaVA status report for the details.

```
https://radio.kasi.re.kr/kava/status_report18b/node3.html.
```

The total available observation time is up to 250 hours including EAVN open use and the observations will be scheduled between 1st September 2019 and 15th January 2020. The maximum observing time per proposal is limited to 100 hours. If requested, the observation time can be allocated over a year, until 1st September 2020, but the observation time will be still limited to 100 hours.

The deadline of submission is at

08:00 UTC on 3rd June, 2019.

Detailed information on the proposal submission can be found at

http://radio.kasi.re.kr/kava/proposal_info.php.

3.2 Proposal Submission

As for the proposal submission, details and application forms of KaVA proposal can be found at the KaVA CfP web site:

http://radio.kasi.re.kr/kava/proposal_kava.php

Any questions on proposal submission should be sent to

eavnprop (at-mark) kasi.re.kr.

Proposals submitted for the 2019B CfP will be reviewed by the referees consisted of KVN and VERA referees already assigned to each array. KaVA makes technical review of all the proposals. The KVN Time Allocation Committee (TAC) and VERA Program Committee (PC) make rating of each KaVA proposal based on the referees, and the KaVA Combined TAC (CTAC) decide the allocation based on each rating result. The results of the review will be announced to PIs in late July, 2019.

3.3 Observation Mode

The K band and the Q band single-frequency single-polarization modes are available and a recording rate of 1024 Mbps (total bandwidth of 256 MHz) will be open for the 2019B CfP. Dual-polarization with KVN and simultaneous multi-frequency mode with KVN will not be available for the 2019B CfP. Two new observation modes are available from the 2016B season; fast antenna nodding mode and 1-beam hybrid (KVN multi-frequency support) mode. Another two new observation modes are available from 2018B season; C2 mode and Wide-field imaging mode. Details are summarized in the Appendix A and B, respectively. From 2019B semester, astrometry observation mode at K-band and C2-mode (backend setup of 128 MHz × 2 channels) are available, as summarized in Appendix D.

3.4 Possible Conflict/duplication with KaVA Large Programs

In order to avoid conflict and/or duplication of the targets with existing KaVA Large Programs, proposers are highly recommended to visit KaVA Large Program (LP) webpage where KaVA LPs and their source list are presented at

http://radio.kasi.re.kr/kava/large_programs.php.

Even though the proposed targets are listed in the LPs, they will be accepted as separate open use observations if the scientific goal of the proposals can not be achieved with the data of LPs. Otherwise, we encourage the proposers to collaborate with the science teams of the corresponding KaVA LPs.

3.5 Target of Opportunity (ToO) Observations

It is strongly recommended that Target of Opportunity proposals (especially expected ToO) are submitted to regular CfP of KaVA. Unexpected or urgent ToO can be submitted to ask Director's time at any time. These proposals must include clear triggering criteria to initiate an observation. The ToO is valid for one year when it is approved. The ToO proposals to Director's time should follow the same format of regular call and should be sent to eavnprop (at-mark) kasi.re.kr.

3.6 Angular Resolution and Largest Detectable Angular Scale

The expected angular resolutions for the K band and the Q band are about 1.2 mas and 0.6 mas, respectively. The synthesized beam size strongly depends on UV coverage,

and could be higher than the values mentioned above because the baselines projected on UV plane become shorter than the distance between antennas. The beam size can be calculated approximately by the following formula;

$$\theta \sim 2063 \left(\frac{\lambda}{[\text{cm}]}\right) \left(\frac{B}{[\text{km}]}\right)^{-1} [\text{mas}].$$
 (2)

where λ and B are observed wavelength in centimeter and the maximum baseline length in kilometer, respectively.

The minimum detectable angular scale for interferometers can be also expressed by equation (2), where the baseline length B is replaced with the shortest one among the array. Because of the relatively short baselines provided by KVN, ~ 300 km, KaVA is able to detect an extended structure up to 9 mas and 5 mas for the K and Q bands, respectively.

3.7 Sensitivity

When a target source is observed, a noise level $\sigma_{\rm bl}$ for each baseline can be expressed as

$$\sigma_{\rm bl} = \frac{2k}{\eta} \frac{\sqrt{T_{\rm sys,1} T_{\rm sys,2}}}{\sqrt{A_{e1} A_{e2}} \sqrt{2B\tau}} = \frac{1}{\eta} \frac{\sqrt{SEFD_{\rm sys,1} SEFD_{\rm sys,2}}}{\sqrt{2B\tau}},\tag{3}$$

where k is Boltzmann constant, η is quantization efficiency (~ 0.88), $T_{\rm sys}$ is system noise temperature, SEFD is system equivalent flux density, A_e is antenna effective aperture area ($A_e = \pi \eta_A D^2/4$ in which A_e and D are the aperture efficiency and antenna diameter, respectively), B is the bandwidth, and τ is on-source integration time. Note that for an integration time beyond 3 minutes (in the K band), the noise level expected by equation (3) cannot be attained because of the coherence loss due to the atmospheric fluctuation. Thus, for finding fringe within a coherence time, the integration time τ cannot be longer than 3 minutes. For VLBI observations, signal-to-noise ratio (S/N) of at least 5 and usually 7 is generally required for finding fringes.

A resultant image noise level $\sigma_{\rm im}$ can be expressed as

$$\sigma_{\rm im} = \frac{1}{\sqrt{\Sigma \sigma_{\rm bl}^{-2}}}. (4)$$

If the array consists of identical antennas, an image noise levels can be expressed as

$$\sigma_{\rm bl} = \frac{2k}{\eta} \frac{T_{\rm sys}}{A_e \sqrt{N(N-1)B\tau}} = \frac{1}{\eta} \frac{SEFD}{\sqrt{N(N-1)B\tau}},\tag{5}$$

where N is the number of antennas. Using the typical antenna parameters (Table 9), baseline and image sensitivity values of KaVA are calculated as listed in Table 10.

Figures 10 and 11 show the system noise temperature at Mizusawa and Ulsan, respectively. For Mizusawa, receiver noise temperatures are also plotted.

Note that the receiver temperature of the VERA antenna includes the temperature increase due to the feedome loss and the spill-over effect. In Mizusawa, typical system temperature in the K band is $T_{\rm sys}=150~{\rm K}$ in fine weather of winter season, but

Table 9: Parameters of each antenna.

KVN						VER	RA
Band	Tsys[K]	η_A	SEFD [Jy]	-	Tsys[K]	η_A	SEFD [Jy]
K	100	0.6	1328		120	0.5	2343
Q	150	0.6	1992		250	0.5	4881

Table 10: Sensitivity of each array.

Baseline sensitivity [mJy]					ge sensit	ivity [mJy]
Band	VERA-VERA	KVN-KVN	VERA-KVN	VERA	KVN	KaVA
K	10.7	6.1	8.1	0.4	0.3	0.2
Q	22.4	9.1	14.3	0.8	0.5	0.3

Sensitivities (1σ) are listed in unit of mJy.

Integration time of 120 seconds and 4 hours are assumed for baseline and image sensitivities, respectively. Total bandwidth of 256 MHz (for continuum emission) is assumed for all the calculations. In the case of narrower bandwidth of 15.625 KHz (for maser emission), sensitivities can be calculated by multiplying a factor of 128.

sometimes rises above $T_{\rm sys}=300~{\rm K}$ in summer season. The system temperature at Iriki station shows a similar tendency to that in Mizusawa. In Ogasawara and Ishigakijima, typical system temperature is similar to that for summer in Mizusawa site, with typical optical depth of $\tau_0=0.2\sim0.3$. The typical system temperature in the Q band in Mizusawa is $T_{\rm sys}=250~{\rm K}$ in fine weather of winter season, and $T_{\rm sys}=300-400~{\rm K}$ in summer season. The typical system temperature in Ogasawara and Ishigakijima in the Q band is larger than that in Mizusawa also.

The typical system temperature in the K band at all KVN stations is around 100 K in winter season. In summer season, it increases up to ~ 300 K. In the Q band, the typical system temperature is around 150 K in winter season and 250 K in summer season at Yonsei and Tamna. The system temperature of Ulsan in the Q band is about 40 K lower than the other two KVN stations. This is mainly due to the difference in receiver noise temperature (see Table 5).

3.8 Calibrator Information

The NRAO VLBA calibrator survey is very useful to search for a continuum source which can be used as a reference source to carry out the delay, bandpass, and phase calibrations. The source list of this calibrator survey can be found at the following VLBA homepage,

http://www.vlba.nrao.edu/astro/calib/index.shtml.

For delay calibrations and bandpass calibrations, calibrators with 1 Jy or brighter are strongly recommended as listed in the VLBA fringe finder survey:

http://www.aoc.nrao.edu/~analysts/vlba/ffs.html.

Interval of observing calibrator scans must be shorter than 1 hour to track the delay and delay rate in the correlation process.

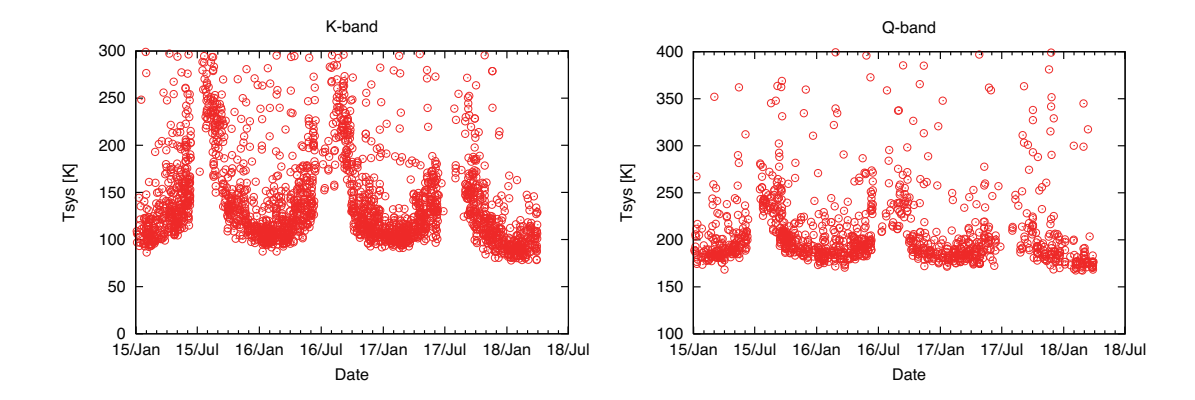


Figure 10: The system noise temperature (red open circles) at the zenith in the K band and the Q band with the Mizusawa antenna.

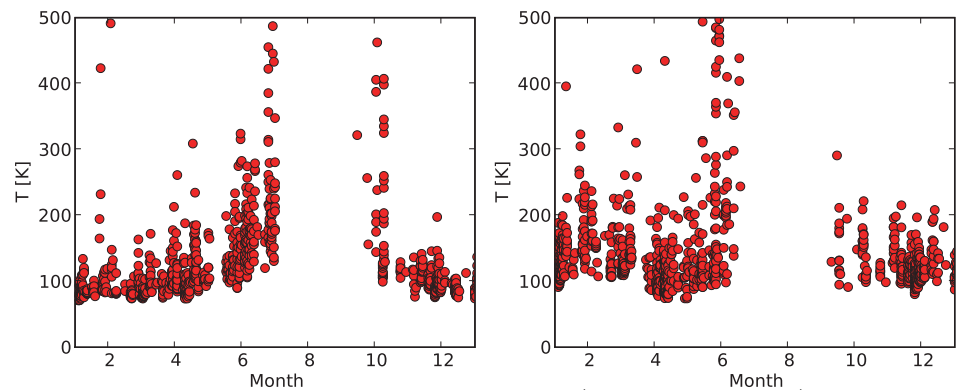


Figure 11: The zenith system noise temperature (red filled circles) at the K band (left) and the Q band (right) in the Ulsan station.

3.9 Date Archive

The users who proposed the observations will have an exclusive access the data for 18 months after the correlation. After that period, all the observed data in the KaVA open use observation will be released as archive data. Thereafter, archived data will be available to any user upon request. This policy is applied to each observation, even if the proposed observation is comprised of multi-epoch observations in this season.

3.10 Recovery Observation

If an open use observation has more than one missing station due to system trouble and/or very severe weather conditions (e.g. strong wind due to a typhoon), the PI can request recovery observations within a year of receiving the correlated data. The PI should resubmit the proposal in which PI should clarify the problems in the previous observations and the necessity of recovery observations for your scientific goal. The KaVA TAC will consider the time allocation of the recovery observations for the next season. If you have any questions, please send an email to kavaprop (at-mark) kasi.re.kr.

4 Observation and Data Reduction

4.1 Preparation

After the acceptance of proposals, users are requested to prepare the observing schedule file two weeks before the observation date. The observer is encouraged to consult a contact person in the KaVA AOC members and/or the assigned support scientist to prepare the schedule file under the support of the contact person and/or the assigned support scientist. The schedule submission should be done by a stand-alone vex file. The examples of KaVA vex file are available at the KaVA web site:

http://radio.kasi.re.kr/kava/kava_observing_preparation.php

On your schedule, we strongly recommend to include at least two fringe finder scans, each lasting 5 or more minutes at the first and latter part of observation in order to search the delay and rate offsets for the correlation.

We request PIs to specify their correlation parameters at the beginning of the vex file for proper correlation processing. In particular, PIs who request for sub-array or dual-beam observations for KaVA should provide a frequency matching table for the correct correlation.

4.2 Observation and Correlation

KaVA members take full responsibility for observation and correlation process, and thus basically proposers will not be asked to take part in observations or correlations. Observations are proceeded by operators from each side (KVN and VERA) and correlated data is delivered to the users in approximately two months including the time for media shipping to KJCC at Daejeon.

After the correlation, the user will be notified where the data can be downloaded by email. After one month later of a correlated data distribution to PIs, disk modules which contains raw observing data can be recycled without notice. Therefore, PIs should investigate the correlated output carefully. For re-correlation or raw data keeping of the data, PI should provide adequate evidence in order to justify his/her request. If there is an issue related to correlated data, PI should consult a support scientist first or the correlator team (kjcc (at-mark) kasi.re.kr), and not to ask KJCC members directly.

4.3 Data Reduction

For the KaVA data reduction, the users are encouraged to reduce the data using the NRAO AIPS software package. The observation data and calibration data will be provided to the users in a format which AIPS can read.

As for the amplitude calibration, we will provide "ANTAB" files which include the system temperature information measured by the R-sky method and the information of the dependence of aperture efficiency on antenna elevation. If the user wants weather information, the information of the temperature, pressure, and humidity during the observation can be provided. In case of questions or problems, the users are encouraged to ask the contact person in KaVA members and/or the assigned support scientist for supports.

4.4 Further Information

The users can contact any staff member of the KaVA by E-mail (see Table 11).

Table 11: Contact addresses.

Name	E-mail address	Related Field
Proposal submission	eavnprop (at-mark) kasi.re.kr	Proposal related requests/questions
User support team	eavnhelp (at-mark) kasi.re.kr	User support in general
Operation team	eavnobs (at-mark) kasi.re.kr	Observation related requests/questions
		schedule submission
Correlator team	kjcc (at-mark) kasi.re.kr	Correlation related requests/questions
		correlated data distribution

References

- [1] KaVA web site: http://kava.kasi.re.kr
- [2] KaVA CfP web site: http://radio.kasi.re.kr/kava/proposal_info.php
- [3] VERA web site: http://veraserver.mtk.nao.ac.jp/index.html
- [4] KVN web site: http://kvn-web.kasi.re.kr/eng
- [5] Han et al. 2013, PASP, 125, 539
- [6] Han et al. 2008, Int. J. Infrared Millimeter Waves, 29, 69
- [7] Lee et al. 2011, PASP, 128, 1398
- [8] Lee et al. 2015, JKAS, 48, 229
- [9] Matsumoto et al. 2014, ApJL, 789, L1
- [10] Niinuma et al. 2014, PASJ, 66, 103
- [11] Oh et al. 2011, PASJ, 63, 1229
- [12] Yun et al. 2016, ApJ, 822, 3
- [13] Proceedings from the 1988 synthesis imaging workshop in NRAO, Chapter 13 in Synthesis Imaging in Radio Astronomy: A Collection of Lectures from the Third NRAO Synthesis Imaging Summer School (http://www.aspbooks.org/a/volumes/table_of_contents/?book_id=118)

A New observation mode from 2016B

Two new observation modes are available from the 2016B season; fast antenna nodding mode and 1-beam hybrid (KVN multi-freuquency support) mode. Details are summarized in the following sections.

A.1 Fast antenna nodding mode

This mode is the conventional mode for VLBI phase reference observations. In this mode, the antenna is nodding between the bright phase calibrator and target source. By fringe fitting of the phase calibrator, the residual phase from the unmodeled clock and atmosphere can be dertermined and then interpolated to the target source to achieve a stable phase of the target source.

With this mode, we can detect and image weak sources, which can not be imaged directly by fringe fitting. This mode will also be used for astrometry to derive accurate position, proper motion and parallax of VLBI targets. From the 2019A season, KaVA is capable of astrometry observations by combining VERA dual-beam mode and KVN fast antenna nodding mode, as described in Appendix C.

A.2 1-beam hybrid (K/Q/W) mode

KaVA will enable us to conduct VLBI observations in combinations of different types of antennas (antenna beams), receiving bands, recording rates (namely total band widths), and filtered base band channels in one observing session, whose cross correlation is still valid for the whole or some parts of KaVA. In such "hybrid" observing modes with KaVA, there are some modes that are available in the 2019B CfP described as follows.

Although VERA shall use only one of dual beams in a single frequency band (K or Q), the KVN is able to observe in two to three of K/Q/W bands simultaneously in a common observing session. Please check the KVN status report for W-band information (http://radio.kasi.re.kr/kvn/status_report_2019). Signal correlation for all the KaVA baselines is valid for the band in which both the KVN and VERA observe, while that for all the observed bands is valid for the KVN baselines.

Frequency allocations should be made separately to the KVN and VERA, including base band channels that are common between the two arrays in a specific band (K or Q). Note that the number of base band channels or the total bandwidth available per frequency band is limited, therefore brighter continuum sources should be selected for group-delay calibration.

Moreover, different frequency-band assignment (K or Q) is also available for each of VERA stations to observe in K/Q-bands simultaneously. In this case, it is necessary to confirm that uv-coverages in both bands are suitable for a target source. For example, suppose a simultaneous observation of faint 44 GHz methanol maser and compact 22 GHz water masers. In this case, VERA Iriki station is assigned to a Q-band observation while other VERA stations are assigned to K-band in addition to a simultaneous K/Q-band observation with the KVN. The Q-band array becomes a compact array consisted with KVN three + VERA Iriki stations, while the K-band array becomes an extended array consisted with KVN three + VERA Mizusawa/Ogasawara/Ishigakijima stations.

B New observation mode from 2018A

Two new observations modes are available from the 2018A semester; C2 mode and Wide-field imaging mode. Details are summarized in the following subsections.

B.1 C2 mode at Q-band

KaVA has provided two correlation modes with 8 IFs × 32 MHz and 16 IFs × 16 MHz, called as the C4 and C5 modes, respectively. To obtain the accurate amplitude values across the all frequency channels, however, the number of basebands (or IFs in AIPS data handling) yielded by the digital filter unit (DFU) is better to be reduced because the amplitude losses mainly occur at the edges of each baseband. This reduction is especially helpful to observe continuum sources, such as active galactic nuclei (AGN). The C2 mode, which has 2 IFs × 128 MHz, therefore, is opened but at only Q-band in 2019B. Note the following two matters: there are some amplitude slopes mainly at VERA stations (Figures 12 and 13 in the VERA status report: http://veraserver.mtk.nao.ac.jp/restricted/CFP2019B/status19B.pdf), which must be corrected by all the gain calibration procedures (AIPS tasks ACCOR, BPASS, and APCAL); multiply the scaling factor to recover the quantization loss (1.3 for Daejeon correlator) [8].

B.2 Wide-field imaging mode

This mode is required to fully image 44 GHz methanol maser emissions associated with star-forming regions, which are generally distributed on the angular scale over 10 arcsec. The wide-field imaging (WFI) mode is achieved with an accumulation period shorter than the usual one of 1.6384 sec in Daejeon correlator at KJCC. Theoretically, the field of view (FoV) within an amplitude loss of 1%, 5%, and 10% is estimated on the basis of the time-average smearing effect due to a finite accumulation period [13]. The FoVs calculated for accumulation periods of 0.2048, 1.6384, and 3.2768 sec are summarized in Table 12, in the case of the highest angular resolution at Q-band of 0.6 mas with KaVA.

TD 11 10 TO TO	1 .	•	1. 1	1 .	1	1 . •	• 1*
Table 12: FoV	within a	ouven	amplitude	loss in	each	accumulation	neriod*
I 00010 12. I 0 V	WIUIIII G		aniphiuac	1000 111	Caci	accultulation	portou .

Accumulation	Aı	nplitude le	OSS
period	1.0%	5.0%	10.0%
(sec)	(arcsec)	(arcsec)	(arcsec)
0.2048	8.6	19.4	27.4
1.6384	1.1	2.4	3.4
3.2768	0.5	1.2	1.7

^{*} Under an assumption of the highest angular resolution at Q-band of 0.6 mas with KaVA.

In the current available specification of Daejeon correlator, there is a trade-off between a shorter accumulation period and a larger number of IF channels to yield higher spectral resolution. The most highly recommended setup is the combination of C2 mode and an accumulation period of 0.2048 sec, in which both a sufficiently high

velocity resolution (0.11 km s⁻¹ for 44 GHz methanol masers) and a sufficiently wide FoV (10 arcsec or more) can be obtained. Thus the recommended set-up for WFI mode is summarized in Table 13.

Table 13: Recommended set-up for WFI mode in the current situation.

Correlation	Sampling	Bandwidth	Accumulation	Spectral
mode	rate	$/\mathrm{IF}$	period	channels/IF
C2	1024 Mbps	128 MHz	$0.2048 \sec$	8,192

The evaluation for the WFI tests was done by the following two ways: comparing the data of an accumulation period of 0.1 sec produced in DiFX to those of 0.2048 sec in Daejeon correlator, and comparing the latter data to the same data but with averaging in 3.2768 sec. These ways provide us a chance to estimate whether such an isolated maser can be detected or not and how much rate of the amplitude loss occurs. The evaluation might be updated on the basis of a comparison between a short-accumulation period data and a multi-tracking center data in the near future.

If you would like to require this WFI mode, please describe your requests in the following two items:

- Requested setting parameters for WFI in the proposal cover sheet
- Reasons for requiring WFI mode in the scientific justification

Finally, note that the file size of correlated data for WFI is as huge as ~600 GByte. We therefore recommend to check and improve the performance of your internet environment and personal computer as high as possible for comfortable data downloading and data processing, respectively. Please refer an example parameters in Table 14:

Table 14: Required performances of internet and personal computer.

Forward speed	$\geq 10 \; \mathrm{MByte \; s^{-1}}$
HDD/SSD volume	$\geq 1.5 \text{ TByte}$
RAM	≥ 16 GByte

Here, the experiment to verify the time-average smearing effect due to a finite accumulation period has been done, however we will also verify the bandwidth smearing effect to KaVA observations in the near future.

C New observation mode from 2019A

New observation mode, phase-referencing mode at K-band, is available from the 2019A semester as a shared-risk mode. Details are summarized in the following subsection.

C.1 Phase referencing mode at K-band

We have confirmed that relative astrometric observation with KaVA can achieve positional accuracies of ~ 20 microarcseconds (μ as) in right ascension and ~ 40 μ as in declination in case of a separation angle of ~ 1 degree between target and phase-reference sources, where K-band (22 GHz) data sets were used for the evaluation (see Fig. 12 and Table 15).

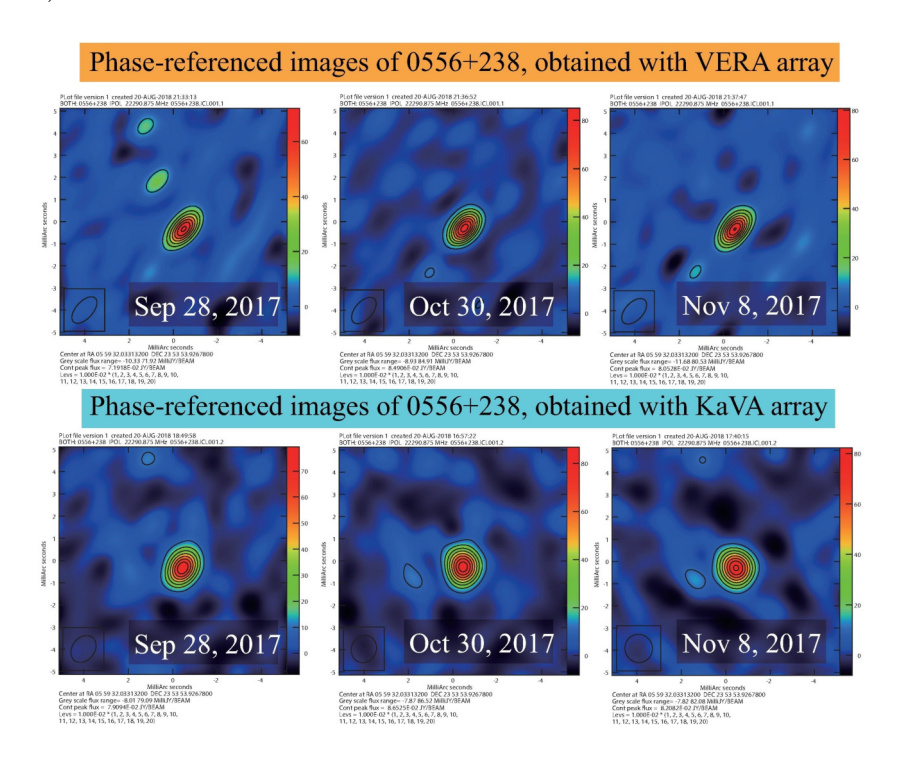


Figure 12: (**Top row**) Phase-referenced images of 0556+238 with VERA, relative to the phase reference source 0601+245. The dates of the observations are September 28th, October 30th and November 8th in 2017 from left to right images. (**Bottom row**) Same as the top row, but for KaVA data used.

C.1.1 VERA dual-beam and KVN single-beam observations

In an astrometric observation, the observation using dual-beam for VERA and single-beam for KVN is recommended. Note that VERA dual-beam system can observe two adjacent objects only with a separation angle between 0.32 and 2.2 degrees at K-band (0.32 and 2.18 for Q-band). Also, it is strongly recommended to observe pair sources with small separation angle (e.g., less than 1 degree) at high elevation (see Table 16). This will reduce the position errors caused by the residuals in atmospheric zenith delay. Note that Table 16 could be used to estimate accuracies of relative astrometry for VERA and KaVA, since the maximum baselines

Table 15: Results of position repeatability for 0556+238.

	1	1	•	
	VE	RA	Ka	VA
Observation date	R.A.	Decl.	R.A.	Decl.
(in 2017)	(μas)	(μas)	(μas)	(μas)
September 28th	-465 ± 15	-332 ± 16	-451 ± 15	-331 ± 15
October 30th	-494 ± 11	-283 ± 12	-462 ± 16	-258 ± 18
November 8th	-505 ± 09	-318 ± 10	-480 ± 13	-287 ± 14
Unweighted mean	-488 ± 21	-311 ± 25	-464 ± 15	-292 ± 37

Column 1 shows the date of observation. Columns 2-3 display image positions of 0556+238, obtained by the phase referencing relative to 0601+245, in right ascension and declination, respectively. Note that the image positions were measured for VERA data. The errors of the positions represent the thermal error, which is typically smaller than a systematic error in ground-based VLBI observation. Columns 4-5 are the same as the Columns 2-3, but for KaVA data used.

Table 16: Simulation results for accuracy of relative astrometry.*

Declination	Position Angles	Separation Angles	$\sigma_{\alpha\cos\delta}$ (mas)	σ_{δ} (mas)
-30°	0°	1°	0.232	0.452
-30°	90°	1°	0.084	0.208
$+15^{\circ}$	0°	1°	0.032	0.029
$+15^{\circ}$	90°	1°	0.050	0.016
$+60^{\circ}$	0°	1°	0.030	0.018
$+60^{\circ}$	90°	1°	0.025	0.028

^{*} Referring to Honma, Tamura & Reid (2008).

Column 1 shows declination of a target source. Columns 2-3 give the position angles east of north of a background (phase reference) source relative to a target source and the separation angles between them. Columns 4-5 list positional errors in right ascension and declination, respectively. Note that the residual in atmospheric zenith delay is assumed to be 2 cm. The error of 2 cm is a typical error in the zenith delay measurements for VERA. The positional errors can be scaled by a separation angle in degrees.

of both arrays are consistent with each other (i.e. positional accuracy of relative astrometry can be given by $\sim \theta_{\rm sep} \frac{c\Delta\tau}{|B|}$ where $\theta_{\rm sep}$ is the separation angle between target and phase reference sources, c is the speed of light, |B| is the baseline length and $\Delta\tau$ is the uncertainty in a delay measurement, see Reid & Honma 2014).

Regarding phase-referencing (antenna switching) cycle for the fast antenna nodding with KVN, users can refer to Table 17.

C.1.2 Tropospheric calibration with GPS and JMA data

Generally, residual atmospheric delay errors dominate cm-wave VLBI positional accuracy. Atmospheric (tropospheric) calibration for VERA is conducted with GPS data, while that for KVN is conducted with Japan Meteorological Agency (JMA) meso-scale analysis data (Hobiger et al. 2008; JMA 2013¹). Nagayama et al. (2015, PASJ, 67, 65) demonstrated that an error of tropospheric zenith delay ($c\Delta\tau_{\rm trop}$) can be suppressed within ~2 cm with both GPS and JMA data.

 $^{^{1}} http://www.jma.go.jp/jma/jma-eng/jma-center/nwp/outline2013-nwp/pdf/outline2013_all.pdf$

Table 17:	Phase-F	Referencing	Cycle	Times	(\min)).*

	Typical weather		Bad weather		Good weather	
	v -					
	($(C_n^{\dagger} = 2 \times 10^7 \text{ m}^{-1/3})$		$4 \times 10^7 \text{ m}^{-1/3}$	$(C_n^{\dagger} = 1 \times 10^7 \text{ m}^{-1/3})$	
	Freque	ency (GHz)	Freque	ency (GHz)	Frequency (GHz)	
EL (deg)	22	$(43)^{\ddagger}$	22	$(43)^{\ddagger}$	22	$(43)^{\ddagger}$
5	0.3	0.2	0.2	0.1	0.8	0.4
10	0.5	0.3	0.2	0.1	0.8	0.6
15	0.7	0.3	0.3	0.1	1.5	0.7
20	0.8	0.4	0.3	0.2	1.8	0.9
25	0.9	0.4	0.4	0.2	2.0	1.0
30	1.0	0.5	0.4	0.2	2.8	1.1
40	1.1	0.5	0.5	0.2	5.8	1.3
50	1.3	0.6	0.6	0.3	9.9	1.5
60	1.8	0.7	0.6	0.3	10.0	2.2
70	2.3	0.7	0.6	0.3	10.0	2.9
80	2.6	0.7	0.6	0.3	10.0	3.3

^{*} Referring to Ulvestad, J., Phase-Referencing Cycle Times, VLBA Scientific Memo 20 (1999).

Column 1 shows antenna elevation angles. Columns 2-3 indicate phase-referencing cycles at 22 and 43 GHz, respectively, under typical weather condition. The phase-referencing cycle is defined as the time between the midpoints of the two calibrator observations before and after the target observation. Columns 4-5 are the same as Columns 2-3, but with bad weather condition (similar to some summer days). Columns 6-7 are the same as Columns 2-3, but with good weather condition (similar to some winter nights).

C.1.3 Delay recalculation table for precise position measurement

The initial delay tracking model at the KJCC correlator is not sufficient for high precision position measurement. Therefore, we provide a calibration table (called as the delay re-calculation table) to PIs, where the necessary information such as a precise geodetic model, the most-updated Earth-rotation parameters, tropospheric and ionospheric delays is included. The table can be loaded with the AIPS task "TBIN".

For this the delivery of data and calibration table will take about three months after the observation.

C.1.4 Digital filter mode

In the relative astrometric observation with KaVA, digital filter mode of "VERA1" (see Table 7) can be used in the case of pair observation of continuum sources (same as Fig. 12). Digital filter mode of "VERA7" or "VERA7MM" (see Table 7) can be used in the case of pair observation of line (e.g. H₂O maser) and continuum sources.

C.1.5 Data reduction

Generally, users are encouraged to carry out data reduction in consultation with contact person and/or support scientist in the KaVA project group. Procedure of astrometric data reduction for VERA data has been summarized in previous papers (e.g. Fig. 11 of Kurayama et al. 2011; Fig. 5 of Imai et al. 2012). Basically, the procedure of data reduction for KaVA data is consistent with that for VERA data, expect for some points.

^{\dagger} C_n is strength of the tropospheric turbulence.

[‡] Now, Q-band phase-referencing mode is not opened.

For instance, parallactic angle should be corrected for KVN array (e.g. with the NRAO AIPS task "CLCOR" combined with the OPCODE = "PANG"), while no need to calibrate the parallactic angle for VERA array (field rotator is equipped in the VERA array).

Since KVN should be operated by fast antenna nodding mode, antenna scan difference between KVN and VERA should be cared in data reduction. For the data reduction, a flag file is generated based on an antenna log and is provided to an observation PI. The AIPS task "UVFLG" can be used to load the flag file.

C.1.6 Note

KVN station coordinates, derived from geodetic VLBI observations, have been unstable with a potential uncertainty of 2–3 cm level, while VERA station coordinates have been determined at 3 mm level (Jike et al. 2009). This potentially degrades the positional accuracy with KaVA although regularly conducted geodetic observations would improve the positional accuracy of KVN station coordinates.

D New observation mode from 2019B

New observation mode, K-band astrometry mode for parallax and proper motion measurements, is available from the 2019B semester as a shared-risk mode. Most of the information, related to the mode, are overlapped with Appendix C. Thus, here we mention only what are not explained in Appendix C.

D.1 K-band astrometry mode for parallax and proper motion measurements

We have confirmed that relative astrometric observation with KaVA can satisfy an expected parallax accuracy, where K-band (22 GHz) data sets were used for the evaluation (see Figures 13 and 14, and Table 18)².

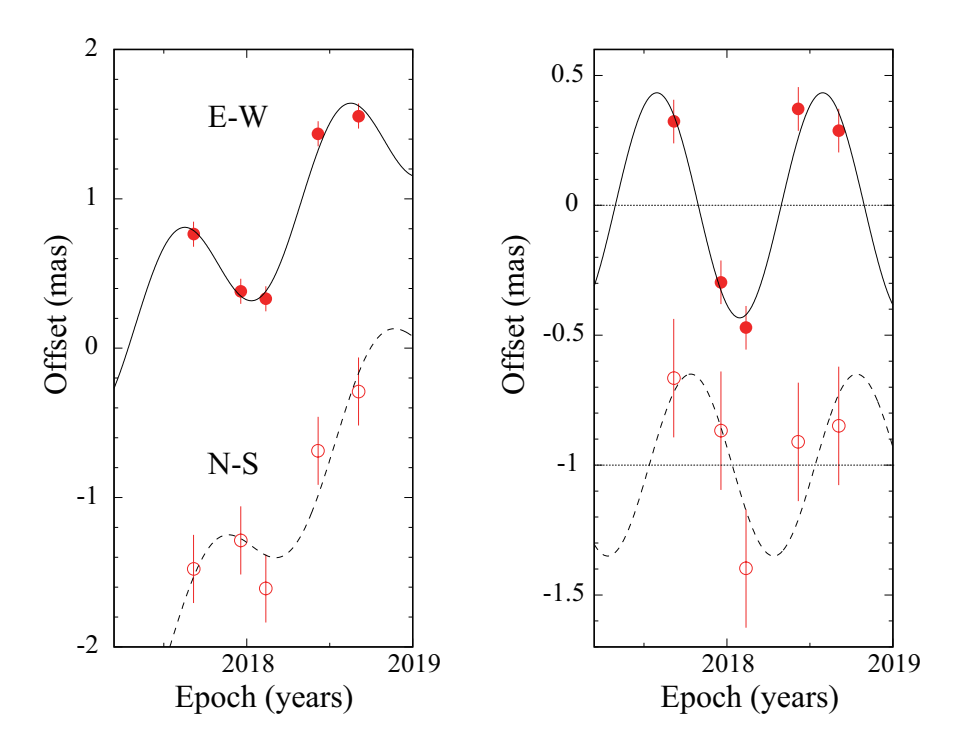


Figure 13: Results of parallax and proper-motion fitting. Plotted are position offset of maser spot (W3OH at $V_{\rm LSR} = -47.5~{\rm km~s^{-1}}$) with respect to the background QSO J0244+6228 (with a separation angle of **2.2 degrees**) toward the east (R.A.cos σ) and north (σ) as a function of time. For clarity, the north direction data is plotted offset from the east direction data. (*Left*) The best-fit models in the east and north directions are shown as continuous and dashed curves, respectively. (*Right*) Same as the Left, but with proper motions removed.

As shown in Table 18, an astrometric positional error in right ascension is ~ 50 microarcseconds (μ as), which is consistent with a theoretical expectation, shown by Table 16 in case of a separation angle of ~ 2 degrees and $\sigma \sim 60^{\circ}$ (i.e. $50-60~\mu$ as). The positional error in declination is much larger than would be expected, which has been

²We cannot guarantee the absolute position accuracy with KaVA in 2019B season, since it's under evaluation and potentially it might have a systematic positional offset with an order of 0.2 mas. Note that "capability of relative astrometry" can be guaranteed in 2019B.

seen in previous VLBI astrometric results and it might be caused by the tropospheric zenith delay residuals (e.g. see Honma et al. 2007).

As mentioned in C.1.5, antenna scan difference between KVN and VERA should be cared in the data reduction because of different on-source time between KVN (fast antenna nodding) and VERA (dual-beam). An example is shown in Fig. 14 where the number of visibility points for baselines including a KVN antenna is smaller than those for baselines of VERA antennas.

		Table 18	<u>8: Parallax r</u>	esults for W3	<u> </u>		
Array	Frequency	Source	$V_{ m LSR}$	Parallax	$\sigma_{\alpha \cos \delta}^*$	σ_{δ}^*	Ref.
	GHz		${\rm km~s^{-1}}$	(mas)	(mas)	(mas)	
KaVA	22	W3OH	-47.5	$0.460 {\pm} 0.035$	0.052	0.256	
VLBA	22	W3OH	$-51.5\sim-48.2$	0.489 ± 0.017	~ 0.050	~ 0.050	(1)

^{*}Positional errors in right ascension and declination were adjusted so that the reduced chi-square becomes unity. Bright and compact maser spot was used for the parallax fit.

Columns 1-2 represent array and observing frequency. Columns 3-4 show source name and LSR velocity of the maser spot, used for the parallax fit. Column 5 displays the parallax result of the source in milli-arcseconds (mas). Columns 6-7 represent the (systematic) positional errors in right ascension and declination, respectively.

Ref. (1) Hachisuka et al. (2006).

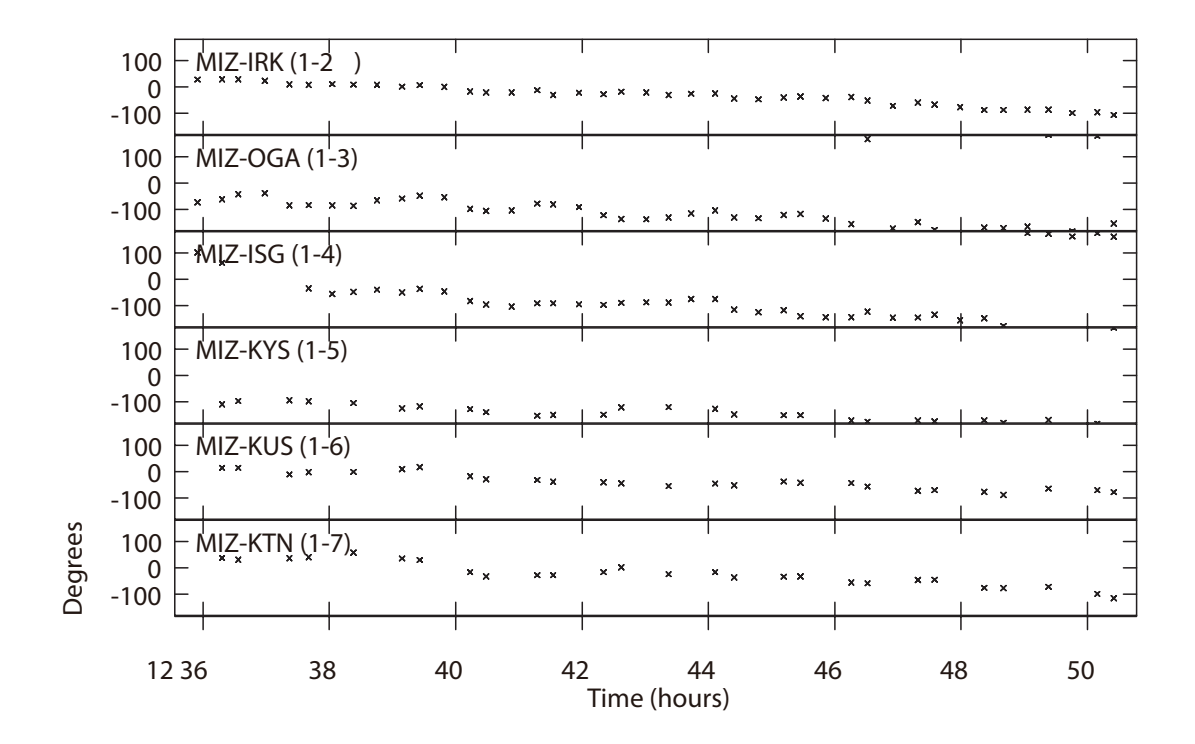


Figure 14: Points represent phase-referenced visibility phase of W3OH (at $V_{LSR} = -47.5 \text{ km s}^{-1}$) with respect to the background QSO J0244+6228 as a function of time. Each point is made with an integration time of 20 seconds. The phases for individual baselines are shown as denoted by an antenna number. The numbers indicate 1:VERA Mizusawa (MIZ); 2:VERA Iriki (IRK); 3:VERA Ogasawara (OGA); 4:VERA Ishigaki (ISG); 5:KVN Yonsei (KYS); 6:KVN Ulsan (KUS); 7:KVN Tamna (KTN).

D.2 C2 mode at K-band

KaVA provides two types of backend modes, 8 intermediate frequency channels (IFs) \times 32 MHz (C4 mode) and 16 IFs \times 16 MHz (C5 mode) from the start of KaVA open-use program in 2014A semester. To obtain the accurate amplitude values across the all IF channels, however, it is better to reduce the number of baseband (or IFs in data handling with AIPS) yielded by the digital filter unit (DFU) so that the amplitude losses at the edge of each baseband are avoided.

KaVA has already provided the backend mode of 2 IFs × 128 MHz (C2 mode) from 2018A semester at only Q-band, as shown in Appendix B.1, and we start providing this mode at K-band from 2019B semester. Note the following two issues: (i) There is a moderate amplitude slope in an IF channel mainly at VERA stations (see Figures 12 and 13 in the VERA status report¹, which must be corrected by all the gain calibration procedures in AIPS (AIPS tasks ACCOR, BPASS, and APCAL): (ii) KaVA's observation data is conventionally correlated by the Daejeon Hardware Correlator. In this case, the scaling factor of 1.3 should be applied to the data to recover the quantization loss² [8].

¹http://veraserver.mtk.nao.ac.jp/restricted/CFP2019B/status19B.pdf

²This scaling factor is conventionally applied to the data using the AIPS task APCAL, however this is not applicable if the data is loaded to AIPS using the AIPS task FITLD with DIGICOR = 3.